

Five years of SGR 1900+14 observations with *BeppoSAX*

P. Esposito^{1,2}, S. Mereghetti², A. Tiengo², L. Sidoli², M. Feroci³, and P. Woods^{4,5}

¹ Università degli Studi di Pavia, Dipartimento di Fisica Nucleare e Teorica and INFN-Pavia, via Bassi 6, I-27100 Pavia, Italy

² INAF - Istituto di Astrofisica Spaziale e Fisica Cosmica Milano, via Bassini 15, I-20133 Milan, Italy

³ INAF - Istituto di Astrofisica Spaziale e Fisica Cosmica Roma, via Fosso del Cavaliere 100, I-00133 Rome, Italy

⁴ Dynetics, Inc., 1000 Explorer Boulevard, Huntsville, AL 35806

⁵ National Space Science and Technology Center, 320 Sparkman Drive, Huntsville, AL 35805

Received 2006 May 3 / Accepted 2006 August 31

Abstract We present a systematic analysis of all the *BeppoSAX* data of the soft gamma-ray repeater SGR 1900+14: these observations allowed us to study the long term properties of the source quiescent emission. In the observation carried out before the 1998 giant flare the spectrum in the 0.8–10 keV energy range was harder and there was evidence for a 20–150 keV emission, possibly associated with SGR 1900+14. This possible hard tail, if compared with the recent *INTEGRAL* detection of SGR 1900+14, has a harder spectrum (power-law photon index ~ 1.6 versus ~ 3) and a 20–100 keV flux ~ 4 times larger. In the last *BeppoSAX* observation (April 2002), while the source was entering the long quiescent period that lasted until 2006, the 2–10 keV flux was $\sim 25\%$ below the historical level. We also studied in detail the spectral evolution during the 2001 flare afterglow. This was characterized by a softening that can be interpreted in terms of a cooling blackbody-like component.

Key words. stars: individual (SGR 1900+14) – stars: neutron – X-rays: stars – X-rays: bursts

1. Introduction

Soft Gamma-ray Repeaters (SGRs) are a small group of high-energy sources, originally discovered through the emission of their characteristic short γ -rays bursts. Only four confirmed SGRs are known, plus two candidates. SGR bursts have typical duration of the order of 0.1 s, peak luminosity in the 10^{39} – 10^{42} erg s $^{-1}$ range, and are emitted during “active” periods that can last from weeks to months. Exceptionally large outbursts are also observed in SGRs. These rare events have properties clearly different from those of the usual short γ -ray bursts. Based on their intensities, they can be classified either as “giant” flares, with total released energy up to 10^{47} erg, or “intermediate” flares, with total energy smaller by orders of magnitude (10^{41} – 10^{43} erg). In the classical X-ray range (~ 1 –10 keV) SGRs are relatively steady sources with luminosity in the 10^{35} – 10^{36} erg s $^{-1}$ range (although fainter states have also been observed, see Kouveliotou et al. 2003 and Mereghetti et al. 2006) and showing periodic pulsations with periods of several seconds and secular spin-down of $\sim 10^{-11}$ – 10^{-10} s s $^{-1}$.

It is generally thought that SGRs, as well as a group of similar pulsars known as Anomalous X-ray Pulsars (AXPs), are magnetars, i.e. isolated neutron stars with strong magnetic fields (see Woods & Thompson 2004 for a review of this class of objects). In the magnetar model both the persistent

X-ray emission and the bursts are powered by magnetic energy (Duncan & Thompson 1992; Thompson & Duncan 1995, 1996). If the secular spin-down observed in SGRs is attributed to dipole radiation losses, as in ordinary radio pulsars, magnetic fields of the order of 10^{14} – 10^{15} G are inferred.

In this paper we focus on SGR 1900+14, reporting all the observations of this source carried out with the *BeppoSAX* satellite. Although some of these data have been already published (Woods et al. 1999a, 2001; Feroci et al. 2003), we reanalyzed all the data sets following the same procedure, in order to compare them in a consistent way. In fact these observations, spanning five years and covering different states of bursting/flaring activity, give the possibility to investigate the long term spectral and flux variability of the source with a homogeneous data set.

In Section 2 we briefly review some results on SGR 1900+14, in the context of the activity history of the source. The spectral and timing analysis are reported in Sections 3 and 4, where we focus on the long term changes in the 1–10 keV emission properties. In Section 5 we report evidence for the detection of SGR 1900+14 in the 20–150 keV band during one of the *BeppoSAX* observations. In Section 6 we concentrate on the spectral variability on short time-scales following the April 2001 intermediate flare.

2. SGR 1900+14: activity episodes and *BeppoSAX* observations

This SGR was discovered in 1979 when a few bursts were recorded with the *Venera 11* and *Venera 12* satellites (Mazets et al. 1979). No other bursts were detected until thirteen years later, when four more events were seen with the BATSE instrument on the *Compton-GRO* satellite in 1992 (Kouveliotou et al. 1993). The X-ray counterpart, discovered with *ROSAT* (Vasisht et al. 1994), was observed a first time with *BeppoSAX* (Woods et al. 1999a). The periodic pulsations in the X-ray counterpart (period of ~ 5.2 s) were discovered with the *ASCA* satellite during an observation in April 1998 (Hurley et al. 1999c), which took place just three weeks before the burst reactivation of the SGR (Hurley et al. 1999b). Subsequent observations with the *Rossi-XTE* satellite confirmed the pulsations and established that the source was spinning down rapidly, with a period derivative of $\sim 10^{-11}$ s s $^{-1}$ (Kouveliotou et al. 1999).

The peak of the bursting activity for SGR 1900+14 was reached on 1998 August 27, when a giant flare was recorded by numerous instruments. This flare started with a short (~ 0.07 s) soft spike (often referred to as the “precursor”), followed by a much brighter hard pulse (duration ~ 1 s) that reached at least $\sim 10^{45}$ erg s $^{-1}$ and a soft γ -ray tail modulated at 5.2 s (Hurley et al. 1999a; Mazets et al. 1999; Feroci et al. 2001). The oscillating tail decayed quasi-exponentially over the next ~ 6 minutes (Feroci et al. 2001). Integrating over the entire flare assuming isotropic emission, at least 10^{44} erg were released in hard X-rays above 15 keV (Mazets et al. 1999). Another bright burst was detected on August 29 (Ibrahim et al. 2001), scaled down by a factor of ~ 100 in peak luminosity and duration, compared to the August 27 flare. The second *BeppoSAX* observation was done less than one month after these events when the source was still active and showed an enhanced X-ray emission (Woods et al. 1999a).

After almost two years of quiescence, during which two *BeppoSAX* observations were carried out (Woods et al. 2001), SGR 1900+14 emitted an intermediate flare on 2001 April 18 (Guidorzi et al. 2001). This event, which prompted the two following *BeppoSAX* observations (Feroci et al. 2003, 2004; Woods et al. 2003), had a duration of ~ 40 s and a total fluence of 1.6×10^{-4} erg cm $^{-2}$. Another bright flare, but of comparatively smaller fluence ($\sim 9 \times 10^{-6}$ erg cm $^{-2}$), occurred after 10 days (Lenters et al. 2003). The last bursts reported from SGR 1900+14, before its recent reactivation (Palmer et al. 2006; Golenetskii et al. 2006) occurred in November 2002 (Hurley et al. 2002).

All the *BeppoSAX* observations of SGR 1900+14 are listed¹ in Table 1. In each observation the SGR was aligned with the optical axis of the instruments. In summary: three observations were triggered by the occurrence of flares (B, E and F), and took place while the source was still active, as testified by the detection of bursts in the *BeppoSAX* data, while all the

other observations can be considered as representative of the source quiescent state emission.

3. Spectral Analysis

The results presented in this section were obtained with the Low Energy Concentrator Spectrometer (LECS) and the Medium Energy Concentrator Spectrometer (MECS) instruments (Parmar et al. 1997; Boella et al. 1997). Both are imaging detectors operating in the 0.1–10 keV and 1.8–10 keV energy ranges respectively.

We used source extraction regions with radii of 4' and 8' for the MECS and the LECS, respectively. Because of the low Galactic latitude of SGR 1900+14, in order to properly account for the presence of the diffuse emission from the Galactic Ridge, concentric rings of 6'.4–9'.6 and 9'–13' were chosen from each pointing for background subtraction with the MECS and the LECS, respectively. The bursts in observations B, E and F were excluded from the analysis². This was done by extracting light curves with a bin size of 1 s and applying intensity filters. All the spectra were rebinned to achieve at least 30 counts in each spectral channel and to oversample by a factor 3 the instrumental energy resolution. The fits were performed simultaneously, over the energy ranges 1.8–10 keV (MECS) and 0.8–4.0 keV (LECS), and including a constant factor to account for normalization uncertainties between the instruments (this factor was constrained to be within its usual range³). Spectral analysis has been performed with the XSPEC v.11.3.2 software package (Arnaud 1996).

In some observations a fit with an absorbed power-law yields unacceptable χ^2 values, therefore we explored a power-law plus blackbody model which gave good fits for all the data sets. Since there is no obvious physical reason for the absorption to change, at least while the source is in quiescence, we fitted all the data sets also with a common value for the N_{H} . The value of 2.6×10^{22} cm $^{-2}$ has been derived fitting simultaneously the spectra of the observations performed while the source was in quiescence. The blackbody temperature (~ 0.4 keV) and emitting area⁴ ($R \sim 6$ –7 km) do not vary much, except during observation E. This observation was performed during the afterglow of the 2001 April 18 flare, and shows clear evidence for spectral variations within the observation (see Section 6). In Figure 1 we have plotted the long term evolution of the flux and spectral parameters obtained in the power-law plus blackbody fits and all the best fit parameters are reported in Table 2. They are consistent with those obtained by Woods et al. 1999a (for observations A and B), Woods et al. 2001 (C and D), and Feroci et al. 2003 (E and F).

The observations in which SGR 1900+14 had the highest X-ray flux are those following the two flares (B and E). The

² The spectral results for the bursts detected in observation E are reported in Feroci et al. (2004).

³ See the Cookbook for *BeppoSAX* NFI Spectral Analysis, <http://www.asdc.asi.it/bepposax/software/cookbook/>

⁴ We assume for SGR 1900+14 a distance of 15 kpc (Vrba et al. 2000).

¹ Observations G and H are listed for completeness, but are of scarce utility due to their short integration time and presence of contaminating sources in the PDS instrument; they will not be discussed further.

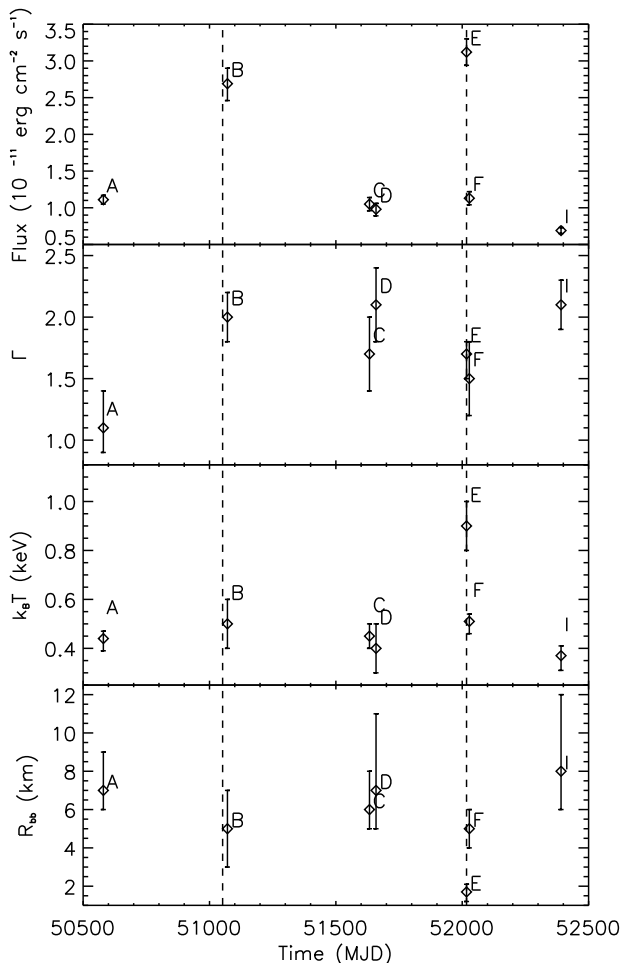


Figure 1. Long term evolution of the 2–10 keV unabsorbed flux and of the spectral parameters of SGR 1900+14 (assuming for the absorption the value of $2.6 \times 10^{22} \text{ cm}^{-2}$). The vertical dashed lines indicate the time of the 1998 August 27 giant flare and of the 2001 April 18 intermediate flare. The error bars are at the 90% confidence level.

flux in the last observation (I), whose analysis is reported here for the first time, is instead $\sim 25\%$ lower than in the other quiescent observations. The fading is also confirmed by a simple comparison of the MECS count rates of observations I and D, which differ at $> 10\sigma$ level. During observation I the transient source XTE J1908+94 (in't Zand et al. 2002), located 24' from the SGR (i.e. just inside the MECS field of view), was in a high state. Therefore we carefully checked our flux estimate for SGR 1900+14 by exploring different background and source extraction regions. Our conclusion is that the observed decrease in the flux is real.

Figure 1 also shows that the power-law component during observation A was slightly harder than in all the following quiescent state observations, performed after the 1998 August 27 giant flare. In order to compare the hardness of the overall spectra of the quiescent observations, we have simultaneously fit them with the same parameters (introducing a normalization factor to account for the flux change) and we note that the spec-

tra C, D, F, and I give an acceptable fit, while the addition of spectrum A makes the simultaneous fit unacceptable, due to the high energy excess shown in figure 2. This means that the pre-flare spectrum was significantly harder than the average quiescent spectrum of SGR 1900+14 measured by *BeppoSAX* after the giant flare.

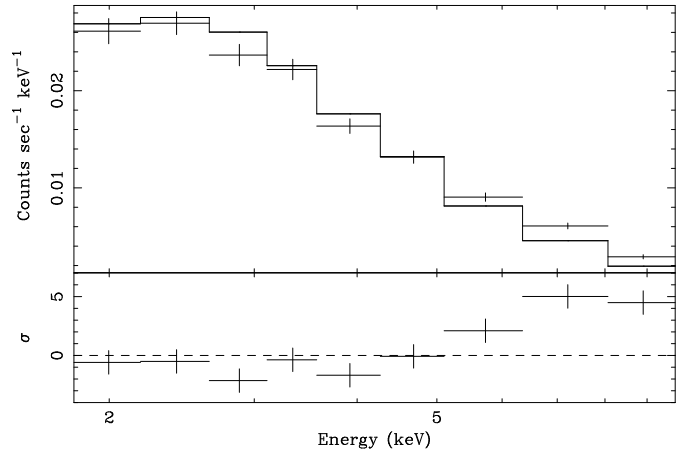


Figure 2. *BeppoSAX*/MECS spectrum of observations A and residuals with respect to the simultaneous fit of the spectra of observation A, C, D, F, and I with an absorbed power-law plus blackbody model with only an overall normalization factor left free to vary. The data have been rebinned graphically to emphasize the trend in the spectral residuals.

4. Timing analysis

For the timing analysis we first corrected the time of arrival of the MECS events to the solar system barycenter, and then used standard folding techniques to measure the source spin period. For observation I we find a period of 5.18019 ± 0.00002 s, and for all the other observations our values (reported in Table 1 and in Figure 1) are in agreement with those of Woods et al. (1999a, 2001) and Feroci et al. (2002). In Figure 3 we show the background-subtracted phase-folded profiles and the pulsed fractions for the seven data sets. We derived the pulsed fractions and the relative errors fitting the pulse profiles with a constant plus one or two (for observation A) sinusoidal functions and computing the ratio between the sin amplitude and the constant. Although SGR 1900+14 has been extensively monitored with the *RXTE* satellite and there are detailed studies of its light curve and pulsed flux evolution (see e.g. Woods et al. 1999b and Göögüs et al. 2002), the results presented here, being obtained with an imaging instrument, have the advantage of providing absolute flux and pulsed fraction measurements.

We note that the changes in the spectrum and in the pulse profile after the giant flare were not accompanied by significant variations in the pulsed fractions. The only significant change has been measured during observation E, when the pulsed fraction was higher ($\sim 25\%$) than the average value of $\sim 17\%$ (this enhancement, related to the afterglow emission, has been

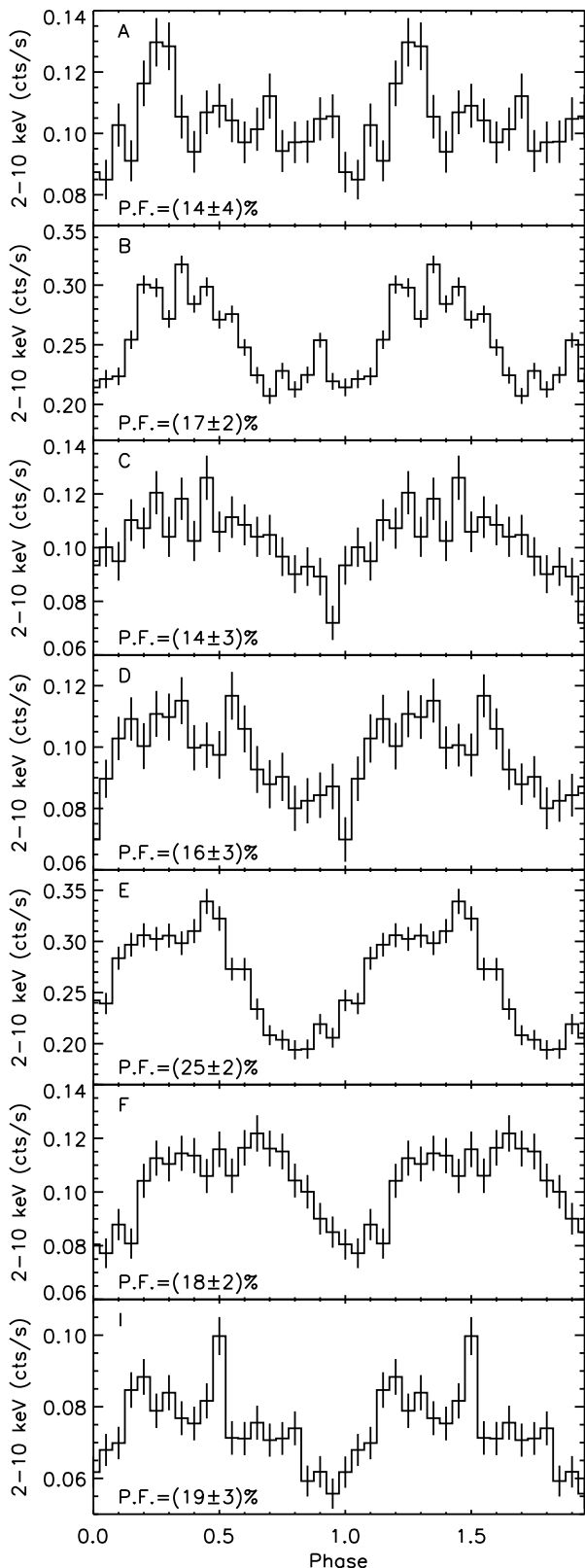


Figure 3. MECS pulse profiles (not phase-connected) and pulsed fraction of SGR 1900+14 in the seven observations (as indicated in the panels).

discussed in Feroci et al. 2003). In contrast the pulse shape of SGR 1806–20, the only other SGR observed before and after a giant flare, was only slightly different after the event, and its pulsed fraction remained small ($\sim 4\%$, Tiengo et al. 2005; Rea et al. 2005) until two months after the flare and then increased to the pre-flare value ($\sim 10\%$, Rea et al. 2005; Woods et al. 2006).

5. Hard X-ray detection

The PDS instrument (Phoswich Detection System, Frontera et al. 1997) extended the spectral and timing capabilities of *BeppoSAX* to the 15–300 keV band. This non-imaging spectrometer had a field of view of 1.3° (FWHM) and the background subtraction was done with a rocking system, which switched between the source and two background regions offset by 3.5° every 96 s.

In all the PDS exposures listed in Table 1 we detected a significant hard X-ray emission. However three transient X-ray sources, the pulsars 4U 1907+97 (Giacconi et al. 1971; Liu et al. 2000) and XTE J1906+09 (Marsden et al. 1998), and the black hole candidate XTE J1908+94 (in't Zand et al. 2002), are located at a small angular distance from SGR 1900+14 ($47'$, $33'$ and $24'$ respectively). When in high state, they can reach fluxes above $\sim 10^{-9}$ erg cm $^{-2}$ s $^{-1}$ in the 20–100 keV range, preventing a sensitive search for a (presumably dimmer) emission from SGR 1900+14. XTE J1908+94 during a bright state is clearly identifiable in the MECS and LECS, since it lies within the field of view of these imaging instruments. This was the case of observation I, performed shortly after the discovery of that source (Woods et al. 2002). The presence of the other two sources has been identified from the detection in the PDS of periodicity at their known pulse periods (~ 89 s for XTE J1906+09 and ~ 440 s for 4U 1907+97) in all the PDS data sets except in the first one. Therefore only for the 1997 observation there is no evidence of contamination from one of these three sources. Given that SGR 1900+14 lies at a low Galactic latitude ($b=0.77^\circ$), we might worry that the flux observed in the PDS during observation A could result from diffuse emission from the Galactic Ridge. Since this emission is constant in time, the lowest count rate observed in later observations (see Table 3) allows us to set an upper limit to its contribution in observation A. This upper limit is of $\sim 60\%$ of the detected flux in the 20–50 keV band and of $\sim 10\%$ in the 50–150 keV band. Although we cannot rule out the possibility of contamination from unknown transient sources, we conclude that the flux measured in observation A up to ~ 150 keV is very likely due to SGR 1900+14.

We extracted the PDS background subtracted spectrum and using the most recent response matrix, we fitted the logarithmically rebinned PDS spectrum in the range 15–150 keV. With a simple power-law model we obtained a photon index $\Gamma = 1.6 \pm 0.3$ and a 20–100 keV flux of $(6 \pm 1) \times 10^{-11}$ erg cm $^{-2}$ s $^{-1}$ with a χ^2 value of 0.98 for 40 d.o.f. We also fitted the PDS spectrum simultaneously with the LECS and MECS spectra, using a blackbody plus power-law model. We included a factor to account for nor-

malisation uncertainties between the low-energy instruments and the PDS. This factor assumed the value of 0.90 (the range of acceptable values is 0.77–0.95). The resulting best fit parameters (photon index $\Gamma = 1.04 \pm 0.08$, blackbody temperature $k_B T = 0.50 \pm 0.06$, radius $R_{bb} = 5 \pm 2$ km, and absorption $N_H = (1.8 \pm 0.5) \times 10^{22} \text{ cm}^{-2}$) are consistent with an extrapolation of the power-law component measured at lower energy (Figure 3.a). We also checked a broken power-law plus blackbody model and, although the improvement in the goodness of the fit, as measured by the F-test statistic, is marginal, we obtained a slightly lower χ^2 value (1.11 for 135 d.o.f. instead of 1.17 for 137 d.o.f.) with a photon index of ~ 0.7 up to ~ 25 keV and of ~ 1.7 above, and with a similar blackbody component (Figure 3.b). Motivated by the structured residuals from ~ 15 keV to ~ 35 keV, where, as discussed above, some contamination from the Galactic diffuse emission cannot be excluded, we performed also a fit using the PDS data only above 35 keV. The resulting parameters are photon index $\Gamma = 1.15 \pm 0.10$, blackbody temperature $k_B T \simeq 0.5$ keV and $R_{bb} \simeq 5$ km, with a χ^2_r value of 1.08 for 123 d.o.f. The 20–100 keV flux derived from all the fits is $(7 \pm 1) \times 10^{-11} \text{ erg cm}^{-2} \text{ s}^{-1}$.

In order to search for pulsations in the hard X-ray range we folded the PDS data at the period of 5.15719 s measured with the MECS, but no significant periodic signal was detected. The 3σ upper limit on the source pulsed fraction derived by a sinusoidal fit is $\approx 50\%$.

Except for observation H, whose high count rate is due to XTE J1908+94⁵, all the post-giant flare observations show a lower count rate in the 50–150 keV band with respect to observation A. The consistent count rates obtained in every observations from the two uncorrelated regions used for background subtractions (see Table 3) assure that this decrease does not result from bright sources in the background pointings. Moreover, the contamination in this band from the X-ray pulsars is expected to be negligible in all observations, since their spectrum in outburst is characterized by a high energy cutoff at 10–15 keV (Wilson et al. 2002; Baykal et al. 2006).

This considerations lead us to conclude that SGR 1900+14 became less bright in the 50–150 keV band after its giant flare. The fact that the 20–50 keV count rate during observation C was lower than in observation A, even though the pulsar XTE J1906+09 was active, might indicate that the flux of SGR 1900+14 in this softer energy band had also significantly decreased.

6. Spectral variability in the afterglow of the 18 April 2001 flare

Flux and spectral variations as a function of time within the individual observations (except for the bursts) were evident, as mentioned above, only for the data collected ~ 7.5 hours after the onset of the 2001 April 18 flare (observation E). While evidence for this based only on hardness ratio analysis was reported in Feroci et al. (2003), here we present, for the first time,

⁵ The source went in outburst in February 2002 and reached its flux peak about two months later (in't Zand et al. 2002).

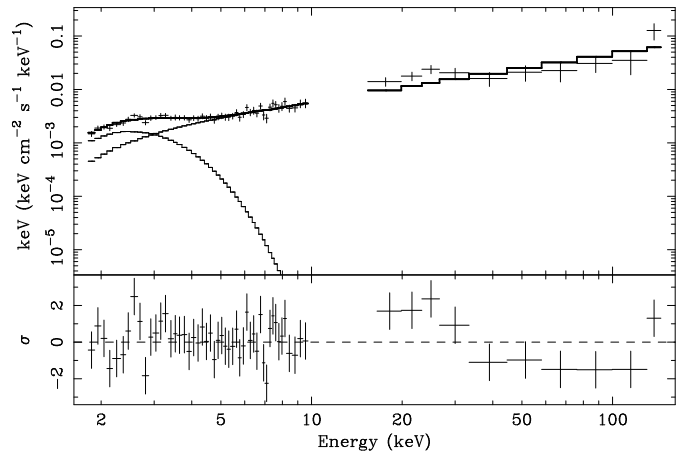


Figure 3. a.

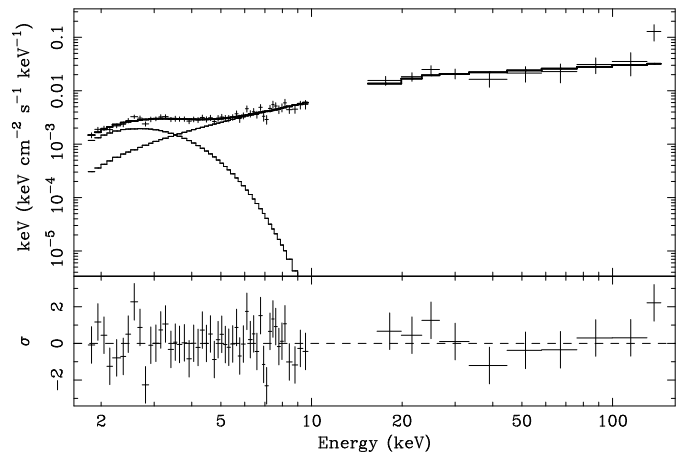


Figure 3. b. Broad band spectrum and residuals from the data of the observation A fitted with a power-law plus blackbody model (a) and with a broken power-law plus blackbody model (b). The data points are from the MECS and PDS instruments and the thick line represents the total model, while the thin lines represent its absorbed power-law and blackbody components.

a time resolved spectral analysis of the afterglow lightcurve.

The SGR 1900+14 light curve for this observation, binned in 5 000 s intervals, is shown in the top panel of Figure 4. A detailed study of the flux decay, using also data from RXTE and Chandra that filled the time gap between observations E and F, has been reported by Feroci et al. (2003). They showed that, after subtracting a constant flux corresponding to the pre-flare quiescent level, the light curve is well described by a power-law with $F \propto t^{-0.9}$, with superimposed a broad “bump” (visible at $t \sim 80 000$ s in Figure 4).

Following this approach, we assumed that the variable “afterglow” emission is present on top of a “quiescent” emission that shows only moderate variations on long time-scales. We therefore extracted the source spectra for five different time intervals (our selection is visible in Figure 4) and fitted them with a model consisting of a power-law plus blackbody with fixed parameters, plus a third variable component to model the afterglow emission. As representative parameters and normalization of the fixed emission we used values consistent with

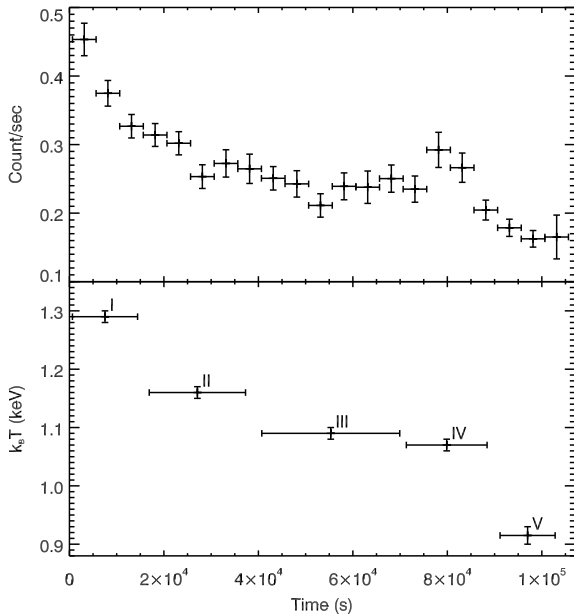


Figure 4. Background subtracted MECS 2–10 keV light curve and blackbody temperature observed on 2001 April 18 about 7.5 hours after the flare. See Table 4 for the latter values, obtained from the addition of a new blackbody component with fixed emitting area. The time intervals with bursts have been excluded. Error bars are at 1σ .

those seen in the last observations before the flare (C and D), i.e. $\Gamma \simeq 2$, $k_B T \simeq 0.4$ keV and $R_{bb} \simeq 7$ km. We found that the variable component was better described by a blackbody than by a power-law (typical χ^2_r values of ~ 1.1 and ~ 1.7 , respectively). The results for the blackbody fits are reported in Table 4. Relatively good fits were also obtained by imposing either a constant temperature or a constant emitting area along the whole observation. The temperatures derived in the latter case (that generally gives lower χ^2 values) are plotted in the bottom panel of Figure 4. These results show that a cooling blackbody emission from a region of constant surface could account for both the flux decrease and the spectral softening observed during the afterglow.

However we note that, due to the relatively low statistics of the time resolved spectra, other spectral decompositions are consistent with the data. One possibility is for example to use the power-law plus blackbody model adopted for the time integrated emission with only either the power-law or the blackbody parameters free to vary.

7. Discussion

Our re-analysis of the *BeppoSAX* data of SGR 1900+14 confirms the spectral variability found in this source by Woods et al. (1999a, 2001), and Feroci et al. (2003) on yearly time-scale. Since they found that in some observations an additional blackbody component was required, we were interested in a more thorough assessment of its possibly persistent presence. Such a two-components spectrum is one of the character-

istics of the AXPs (Mereghetti et al. 2002) and has also been observed in the other well studied soft gamma-ray repeater SGR 1806–20 (Mereghetti et al. 2005b). Although formally required only in two (possibly three) observations, that component might well be a permanent feature, always present in this source. In fact, except during the aftermath of the April 2001 flare, its temperature (~ 0.4 keV) and emitting area (~ 6 – 7 km) are consistent with all the spectra. If we assume an underlying and nearly steady blackbody, it might be that, as proposed by Woods et al. 1999a and Kouveliotou et al. 2001, this spectral component is visible only in the observations that offer both a low power-law flux and good statistics.

The long term spectral variability seems to correlate with the occurrence of the giant and intermediate flares and, in a more complex way, with the ordinary bursting activity. Comparing the only *BeppoSAX* pre-flare observation with the quiescent post-flare ones, there is evidence for a softening in the spectrum. Also SGR 1806–20 after its 2004 December 27 giant flare displayed a softer spectrum with respect to the 2004 levels (Rea et al. 2005). This is qualitatively consistent with the magnetar scenario, in which the spectral hardening is linked to the increasing torque of the twisted magnetosphere, that finally drives the SGR to a giant flare (Thompson et al. 2002; Mereghetti et al. 2005b). Then, after the flare, the source magnetosphere is foreseen to relax into a less twisted configuration, with a softer spectrum.

The most recent *BeppoSAX* observation of SGR 1900+14 (Observation I, April 2002), shows a small but statistically significant fading compared to the preceding observations. A long term monotonic decrease of the X-ray emission has been observed in SGR 1627–41 (Kouveliotou et al. 2003; Mereghetti et al. 2006) from 1998 to 2004. During this period no bursts were recorded from SGR 1627–41, and its fading has been interpreted as due to the cooling of the neutron star surface after the heating occurred when the source was active in 1998. SGR 1900+14 was still moderately active during 2002 (Hurley et al. 2002), but then no bursts were observed for several years. The smaller luminosity in the last *BeppoSAX* observation might thus correspond to the initial part of a cooling and fading phase, at least qualitatively similar to that observed in SGR 1627–41, but now interrupted by the recent (March 2006) reactivation (Palmer et al. 2006; Golenetskii et al. 2006).

During the afterglow of the 2001 April 18 flare, Feroci et al. (2003) found a flux decrease and a spectral softening. Our re-analysis shows that the variable spectral component can be well modeled as an additional blackbody emitted from a smaller and hotter (but rapidly cooling) region of the neutron star surface. Successful attempts to explain observations of afterglow flux decays in magnetars by means of a cooling thermal component are described in Ibrahim et al. (2001), Lenters et al. (2003), and Woods et al. (2004); all these works point out evidence of cooling hot spots on the surface of the neutron star exposed to a fireball. However we note that the occurrence of the bump in the light curve of the afterglow is an anomaly in the picture of the cooling of a thermal emission, since it requires a re-injection of energy; we refer to Feroci et al. 2003 for an extensive discussion of this issue.

Evidence for persistent emission above 20 keV for

SGR 1900+14 has recently been obtained with *INTEGRAL* observations (Götz et al. 2006). We found that a hard tail was visible also in the 1997 *BeppoSAX* PDS data. If this emission is indeed due to SGR 1900+14, our 50 ks long observation indicates significant differences with respect to the average properties obtained with *INTEGRAL*, based on the sum of many observations performed discontinuously from March 2003 to June 2004. The PDS 20–100 keV flux is ~ 4 times larger⁶ and the spectrum is harder (photon index ~ 1.1) than that measured with *INTEGRAL* (photon index ~ 3). Even considering our fit based only on the PDS instrument, the difference in the hard X-ray spectral index is significant (photon index ~ 1.6 versus ~ 3). Another interesting indication from the PDS data is a decrease of the 50–150 keV flux of SGR 1900+14 after the giant flare: it is possible that the hard X-ray flux decrease and softening in SGR 1900+14 was a consequence of the 1998 August 27 giant flare.

The only other SGR established as a persistent hard X-ray source to date is SGR 1806–20 (Mereghetti et al. 2005a; Molkov et al. 2005). For this source observations carried out with *XMM-Newton* in the April 2003–October 2004 period, showed a progressive spectral hardening in the 1–10 keV band, as the source increased its burst rate before the giant flare (Mereghetti et al. 2005b). The *INTEGRAL* observations displayed some evidence of a similar behaviour above 20 keV. In fact its photon index varied from ~ 1.9 in the period March 2003–April 2004 to ~ 1.5 in September–October 2004 (Mereghetti et al. 2005a). A comparison of the hard X-ray luminosity of the two SGRs in the “pre-flare” state is subject to uncertainties in their distances. For SGR 1900+14 a distance of 15 kpc has been derived based on its likely association with a young star cluster (Vrba et al. 2000), while for SGR 1806–20 the distance is rather debated and has been variously estimated from 6.4 kpc to 15 kpc (Cameron et al. 2005; McClure-Griffiths & Gaensler 2005). If we assume a distance of 15 kpc for both sources we obtain similar 20–100 keV luminosities: $(1.5 \pm 0.3) \times 10^{36}$ erg s $^{-1}$ for SGR 1900+14 and $(1.2 \pm 0.1) \times 10^{36}$ erg s $^{-1}$ for SGR 1806–20.

These results, together with the recent detections of several AXPs in the hard X-ray range (Molkov et al. 2004; Kuiper et al. 2004; Revnivtsev et al. 2004; den Hartog et al. 2006; Kuiper et al. 2006) with 20–100 keV luminosities similar or larger than those below 10 keV, indicate that non thermal magnetospheric phenomena are energetically important in magnetars. Soft X-rays give only a partial view and broad band observations are required for a better understanding of the physical processes occurring in these sources. In this respect, SGR 1900+14 being probably the first magnetar showing evidence for variability in the hard X-ray range and currently in a moderately active state, is a good target to further explore possible correlations between the persistent emission and the bursting activity.

Acknowledgements.

⁶ The uncertainty in the relative calibration of the two satellite in the energy band considered here is of $\approx 10\%$ (Kirsch et al. 2005).

This work has been partially supported by the Italian Space Agency and by the Italian Ministry for Education, University and Research (grant PRIN-2004023189). The authors are grateful to the anonymous referee whose valuable comments led to substantial improvements in the paper.

References

Arnaud, K. A. 1996, in ASP Conf. Ser. 101: Astronomical Data Analysis Software and Systems V, ed. G. H. Jacoby & J. Barnes

Baykal, A., İnam, S. Ç., & Beklen, E. 2006, MNRAS, 369, 1760

Boella, G., Chiappetti, L., Conti, G., et al. 1997, A&AS, 122, 327

Cameron, P. B., Chandra, P., Ray, A., et al. 2005, Nature, 434, 1112

den Hartog, P. R., Hermsen, W., Kuiper, L., et al. 2006, A&A, 451, 587

Duncan, R. C. & Thompson, C. 1992, ApJ, 392, L9

Feroci, M., Calandro, G. A., Massaro, E., Mereghetti, S., & Woods, P. M. 2004, ApJ, 612, 408

Feroci, M., Hurley, K., Duncan, R. C., & Thompson, C. 2001, ApJ, 549, 1021

Feroci, M., Mereghetti, S., Costa, E., et al. 2002, in ASP Conf. Ser. 271: Neutron Stars in Supernova Remnants, ed. P. O. Slane & B. M. Gaensler, [ArXiv: astro-ph/0112239]

Feroci, M., Mereghetti, S., Woods, P., et al. 2003, ApJ, 596, 470

Frontera, F., Costa, E., dal Fiume, D., et al. 1997, A&AS, 122, 357

Giacconi, R., Kellogg, E., Gorenstein, P., Gursky, H., & Tananbaum, H. 1971, ApJ, 165, L27

Golenetskii, S., Aptekar, R., Mazets, E., et al. 2006, GRB Circular Network, 4936

Götz, D., Mereghetti, S., Tiengo, A., & Esposito, P. 2006, A&A, 449, L31

Göğüş, E., Kouveliotou, C., Woods, P. M., Finger, M. H., & van der Klis, M. 2002, ApJ, 577, 929

Guidorzi, C., Montanari, E., Frontera, F., et al. 2001, GRB Coordinates Network, 1041, 1

Hurley, K., Cline, T., Mazets, E., et al. 1999a, Nature, 397, 41

Hurley, K., Kouveliotou, C., Woods, P., et al. 1999b, ApJ, 510, L107

Hurley, K., Li, P., Kouveliotou, C., et al. 1999c, ApJ, 510, L111

Hurley, K., Mazets, E., Golenetskii, S., & Cline, T. 2002, GRB Coordinates Network, 1715

Ibrahim, A. I., Strohmayer, T. E., Woods, P. M., et al. 2001, ApJ, 558, 237

in't Zand, J. J. M., Miller, J. M., Oosterbroek, T., & Parmar, A. N. 2002, A&A, 394, 553

Kirsch, M. G., Briel, U. G., Burrows, D., et al. 2005, in UV, X-Ray, and Gamma-Ray Space Instrumentation for Astronomy XIV. Edited by Siegmund, Oswald H. W. Proceedings of the SPIE, Volume 5898, pp. 22–33, [ArXiv: astro-ph/0508235]

Kouveliotou, C., Eichler, D., Woods, P. M., et al. 2003, ApJ, 596, L79

Kouveliotou, C., Fishman, G. J., Meegan, C. A., et al. 1993, *Nature*, 362, 728

Kouveliotou, C., Strohmayer, T., Hurley, K., et al. 1999, *ApJ*, 510, L115

Kouveliotou, C., Tennant, A., Woods, P. M., et al. 2001, *ApJ*, 558, L47

Kuiper, L., Hermsen, W., den Hartog, P. R., & Collmar, W. 2006, *ApJ*, 645, 556

Kuiper, L., Hermsen, W., & Mendez, M. 2004, *ApJ*, 613, 1173

Lenters, G. T., Woods, P. M., Goupell, J. E., et al. 2003, *ApJ*, 587, 761

Liu, Q. Z., van Paradijs, J., & van den Heuvel, E. P. J. 2000, *A&AS*, 147, 25

Marsden, D., Gruber, D. E., Heindl, W. A., Pelling, M. R., & Rothschild, R. E. 1998, *ApJ*, 502, L129+

Mazets, E. P., Cline, T. L., Aptekar', R. L., et al. 1999, *Astronomy Letters*, 25, 635

Mazets, E. P., Golenetskii, S. V., & Guryan, Y. A. 1979, *Soviet Astronomy Letters*, 5, 343

McClure-Griffiths, N. M. & Gaensler, B. M. 2005, *ApJ*, 630, L161

Mereghetti, S., Chiarlone, L., Israel, G. L., & Stella, L. 2002, in *Neutron Stars, Pulsars, and Supernova Remnants*, ed. W. Becker, H. Lesch & J. Trümper, [ArXiv: astro-ph/0205122]

Mereghetti, S., Esposito, P., Tiengo, A., et al. 2006, *A&A*, 450, 759

Mereghetti, S., Götz, D., Mirabel, I. F., & Hurley, K. 2005a, *A&A*, 433, L9

Mereghetti, S., Tiengo, A., Esposito, P., et al. 2005b, *ApJ*, 628, 938

Molkov, S., Hurley, K., Sunyaev, R., et al. 2005, *A&A*, 433, L13

Molkov, S. V., Cherepashchuk, A. M., Lutovinov, A. A., et al. 2004, *Astronomy Letters*, 30, 534

Palmer, D., Sakamoto, T., Barthelmy, S., et al. 2006, *The Astronomer's Telegram*, 789

Parmar, A. N., Martin, D. D. E., Bvdaz, M., et al. 1997, *A&AS*, 122, 309

Rea, N., Tiengo, A., Mereghetti, S., et al. 2005, *ApJ*, 627, L133

Revnivtsev, M. G., Sunyaev, R. A., Varshalovich, D. A., et al. 2004, *Astronomy Letters*, 30, 382

Thompson, C. & Duncan, R. C. 1995, *MNRAS*, 275, 255

Thompson, C. & Duncan, R. C. 1996, *ApJ*, 473, 322

Thompson, C., Lyutikov, M., & Kulkarni, S. R. 2002, *ApJ*, 574, 332

Tiengo, A., Esposito, P., Mereghetti, S., et al. 2005, *A&A*, 440, L63

Vasisht, G., Kulkarni, S. R., Frail, D. A., & Greiner, J. 1994, *ApJ*, 431, L35

Vrba, F. J., Henden, A. A., Luginbuhl, C. B., et al. 2000, *ApJ*, 533, L17

Wilson, C. A., Finger, M. H., Gögüş, E., Woods, P. M., & Kouveliotou, C. 2002, *ApJ*, 565, 1150

Woods, P. M., Kaspi, V. M., Thompson, C., et al. 2004, *ApJ*, 605, 378

Woods, P. M., Kouveliotou, C., Finger, M. H., et al. 2002, *IAU Circ.*, 7856, 1

Woods, P. M., Kouveliotou, C., Finger, M. H., et al. 2006, Submitted to *ApJ*, [ArXiv: astro-ph/0602402]

Woods, P. M., Kouveliotou, C., Gögüş, E., et al. 2003, *ApJ*, 596, 464

Woods, P. M., Kouveliotou, C., Gögüş, E., et al. 2001, *ApJ*, 552, 748

Woods, P. M., Kouveliotou, C., van Paradijs, J., Finger, M. H., & Thompson, C. 1999a, *ApJ*, 518, L103

Woods, P. M., Kouveliotou, C., van Paradijs, J., et al. 1999b, *ApJ*, 524, L55

Woods, P. M. & Thompson, C. 2004, in "Compact Stellar X-ray Sources", ed. W.H.G. Lewin and M. van der Klis, [ArXiv: astro-ph/0406133]

Table 1. Summary of the *BeppoSAX* observations of SGR 1900+14 .

Obs.	Date	MJD	LECS exposure	MECS exposure	PDS exposure	Period
A	1997-05-12	50580	19.9 ks	45.8 ks	20.1 ks	5.15719 ± 0.00003 s
B	1998-09-15	51071	13.8 ks	33.3 ks	15.8 ks	5.16026 ± 0.00002 s
C	2000-03-30	51633	14.4 ks	40.3 ks	18.3 ks	5.16709 ± 0.00003 s
D	2000-04-25	51659	17.4 ks	40.5 ks	18.8 ks	5.16765 ± 0.00003 s
E	2001-04-18	52017	20.4 ks	46.4 ks	16.7 ks	5.17277 ± 0.00001 s
F	2001-04-29	52028	25.7 ks	57.6 ks	25.6 ks	5.17298 ± 0.00001 s
G	2001-11-05	52218	–	1.3 ks	0.5 ks	–
H	2002-03-09	52342	–	–	47.6 ks	–
I	2002-04-27	52391	–	82.9 ks	–	5.18019 ± 0.00002 s

Table 2. Summary of the spectral results in the 0.8–10 keV energy range. Errors are given at the 90% confidence level.

Obs.	Model	N_{H} (10^{22} cm^{-2})	Γ	$k_B T$ (keV)	R_{bb}^a (km)	Flux ^b ($10^{-11} \text{ erg cm}^{-2} \text{ s}^{-1}$)	χ^2_r (d.o.f.)
A	PL	1.4 ± 0.2	1.9 ± 0.1	–	–	$0.92_{-0.03}^{+0.04}$	1.60 (98)
	PL+BB	$1.6_{-0.4}^{+0.6}$	$0.9_{-0.4}^{+0.3}$	0.5 ± 0.1	4_{-1}^{+2}	1.0 ± 0.1	1.12 (96)
	PL+BB	2.6 (fixed)	$1.1_{-0.2}^{+0.3}$	$0.44_{-0.05}^{+0.03}$	7_{-1}^{+2}	1.11 ± 0.06	1.16 (97)
B	PL	2.4 ± 0.2	2.2 ± 0.1	–	–	2.6 ± 0.1	1.22 (113)
	PL+BB	$1.7_{-0.5}^{+0.6}$	$1.5_{-0.6}^{+0.5}$	0.7 ± 0.1	3 ± 1	2.5 ± 0.2	1.16 (111)
	PL+BB	2.6 (fixed)	2.0 ± 0.2	0.5 ± 0.1	5 ± 2	2.7 ± 0.2	1.21 (112)
C	PL	$2.0_{-0.3}^{+0.4}$	2.3 ± 0.1	–	–	0.95 ± 0.04	1.29 (84)
	PL+BB	2 ± 1	$1.7_{-0.6}^{+0.3}$	0.5 ± 0.1	5_{-2}^{+7}	$1.0_{-0.2}^{+0.1}$	1.09 (82)
	PL+BB	2.6 (fixed)	1.7 ± 0.3	0.45 ± 0.05	6_{-1}^{+2}	1.1 ± 0.1	1.08 (83)
D	PL	2.1 ± 0.3	2.4 ± 0.1	–	–	0.90 ± 0.05	1.06 (83)
	PL+BB	$2.2_{-0.7}^{+0.9}$	$2.0_{-0.5}^{+0.4}$	0.5 ± 0.1	4_{-2}^{+8}	$0.9_{-0.2}^{+0.1}$	1.00 (81)
	PL+BB	2.6 (fixed)	2.1 ± 0.3	0.4 ± 0.1	7_{-2}^{+4}	1.0 ± 0.1	0.99 (82)
E	PL	3.6 ± 0.2	2.2 ± 0.1	–	–	3.5 ± 0.1	1.18 (121)
	PL+BB	$2.6_{-0.9}^{+0.7}$	$1.8_{-0.8}^{+0.3}$	$0.9_{-0.1}^{+0.2}$	$1.6_{-0.8}^{+0.6}$	$3.1_{-0.2}^{+0.3}$	1.13 (119)
	PL+BB	2.6 (fixed)	$1.7_{-0.2}^{+0.1}$	0.9 ± 0.1	$1.7_{-0.5}^{+0.4}$	3.1 ± 0.2	1.12 (120)
F	PL	$2.4_{-0.2}^{+0.3}$	2.3 ± 0.1	–	–	$1.06_{-0.03}^{+0.04}$	1.35 (105)
	PL+BB	$2.4_{-0.5}^{+0.8}$	1.4 ± 0.4	0.5 ± 0.1	5_{-1}^{+3}	$1.1_{-0.2}^{+0.1}$	1.06 (103)
	PL+BB	2.6 (fixed)	1.5 ± 0.3	$0.51_{-0.05}^{+0.03}$	5 ± 1	1.1 ± 0.1	1.05 (104)
I	PL	1.9 ± 0.3	2.4 ± 0.1	–	–	0.62 ± 0.03	1.06 (94)
	PL+BB	3 ± 1	2.2 ± 0.3	0.3 ± 0.1	8_{-4}^{+25}	$0.73_{-0.09}^{+0.04}$	0.94 (92)
	PL+BB	2.6 (fixed)	2.1 ± 0.2	$0.37_{-0.06}^{+0.04}$	8_{-2}^{+4}	0.69 ± 0.04	0.93 (93)

^a Radius at infinity assuming a distance of 15 kpc.^b Flux in the 2–10 keV range, corrected for the absorption.**Table 3.** PDS count rates for the ‘off’ and ‘on’ source positions during the observations of SGR 1900+14 . Errors are given at 1 σ .

Region	Energy band (keV)	Obs. A (cts/s)	Obs. B (cts/s)	Obs. C (cts/s)	Obs. D (cts/s)	Obs. E (cts/s)	Obs. F (cts/s)	Obs. H (cts/s)
OFF –	20–50	4.88 ± 0.02	4.67 ± 0.02	3.75 ± 0.01	3.69 ± 0.01	3.37 ± 0.01	3.38 ± 0.01	3.35 ± 0.01
	50–150	6.87 ± 0.02	6.51 ± 0.02	5.23 ± 0.02	5.27 ± 0.02	4.75 ± 0.01	4.75 ± 0.01	4.73 ± 0.01
OFF +	20–50	4.91 ± 0.02	4.67 ± 0.02	3.74 ± 0.02	3.71 ± 0.01	3.38 ± 0.01	3.40 ± 0.01	3.35 ± 0.01
	50–150	6.83 ± 0.02	6.44 ± 0.02	5.24 ± 0.02	5.21 ± 0.02	4.76 ± 0.01	4.78 ± 0.01	4.75 ± 0.01
ON ^a	20–50	0.27 ± 0.03	0.79 ± 0.04	0.11 ± 0.03	0.36 ± 0.03	0.45 ± 0.03	0.43 ± 0.02	9.33 ± 0.02
	50–150	0.21 ± 0.04	0.12 ± 0.04	< 0.03	< 0.02	0.11 ± 0.03	0.06 ± 0.03	4.48 ± 0.02

^a Background subtracted values.

Table 4. Time resolved spectral results for observation E. The table gives the parameters of a blackbody component added to a fixed component with $N_{\text{H}} = 2.6 \times 10^{22} \text{ cm}^{-2}$, $\Gamma = 2$, $k_B T = 0.4 \text{ keV}$, and $R_{bb} = 7 \text{ km}$ (see Section 6 for details). Errors are given at 1σ .

Time interval	$k_B T$ (keV)	R_{bb}^a (km)	χ^2_r (d.o.f.)
I	$1.23^{+0.02}_{-0.03}$	1.8 ± 0.1	1.03 (69)
	1.1 (fixed)	$2.17^{+0.03}_{-0.02}$	1.35 (70)
	1.29 ± 0.01	1.6 (fixed)	1.09 (70)
II	$1.15^{+0.03}_{-0.02}$	1.6 ± 0.1	1.21 (74)
	1.1 (fixed)	$1.77^{+0.02}_{-0.03}$	1.24 (75)
	1.16 ± 0.01	1.6 (fixed)	1.20 (75)
III	1.16 ± 0.04	1.4 ± 0.1	0.98 (64)
	1.1 (fixed)	$1.56^{+0.02}_{-0.03}$	1.01 (65)
	1.09 ± 0.01	1.6 (fixed)	1.04 (65)
IV	1.10 ± 0.05	$1.5^{+0.2}_{-0.1}$	1.31 (45)
	1.1 (fixed)	1.50 ± 0.03	1.28 (46)
	1.07 ± 0.01	1.6 (fixed)	1.29 (46)
V	0.94 ± 0.07	$1.5^{+0.3}_{-0.2}$	1.25 (29)
	1.1 (fixed)	1.09 ± 0.04	1.35 (30)
	$0.92^{+0.01}_{-0.02}$	1.6 (fixed)	1.21 (30)

^a Radius at infinity assuming a distance of 15 kpc.